Supplementary material
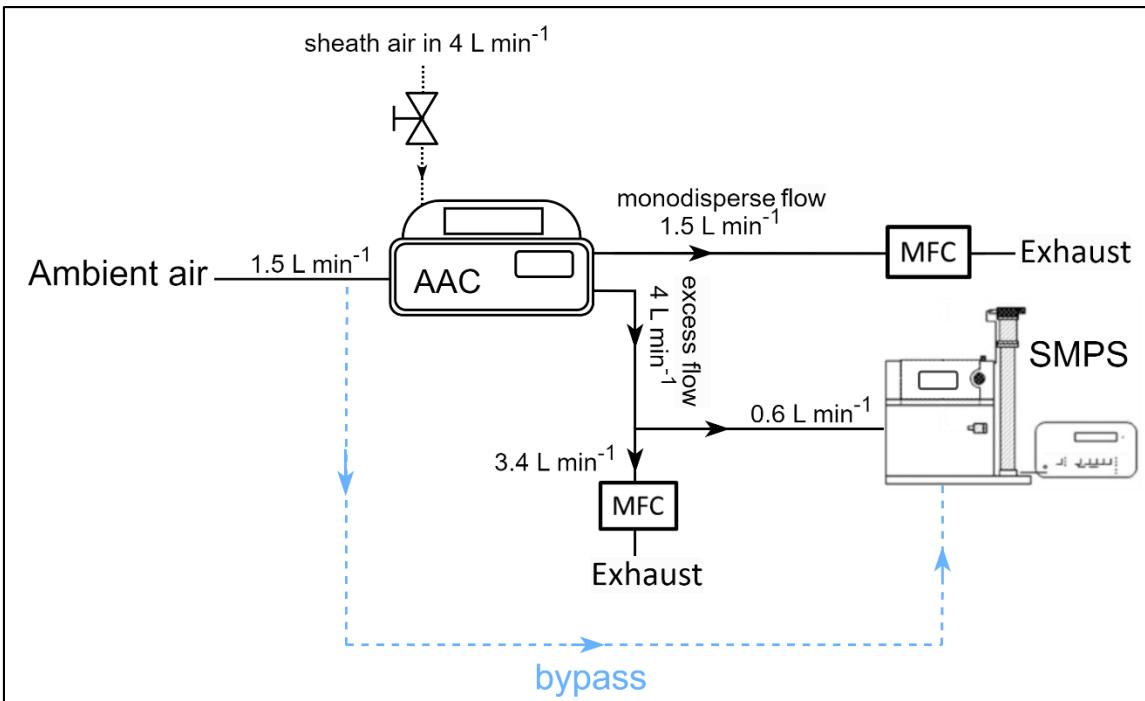
Figure S1. Experimental set-up for the testing of the AAC as a $PM_{0.1}$ cut-off using ambient air. This setup was used to evaluate the system's cut-off sharpness, dilution, and particle losses within the AAC.
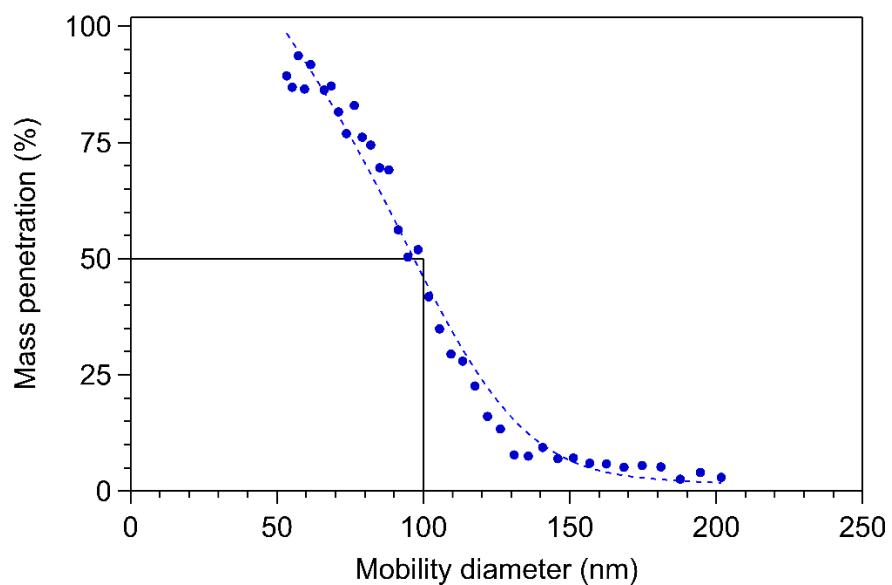
Figure S2. Mass penetration percentage of $PM_{0.1}$ measured by the SMPS for the experimental set-up of Figure S1. The dashed line represents the best-fitting curve. The black lines show that the cut diameter (d_{50}), where there is 50% mass penetration, is at 100 nm.
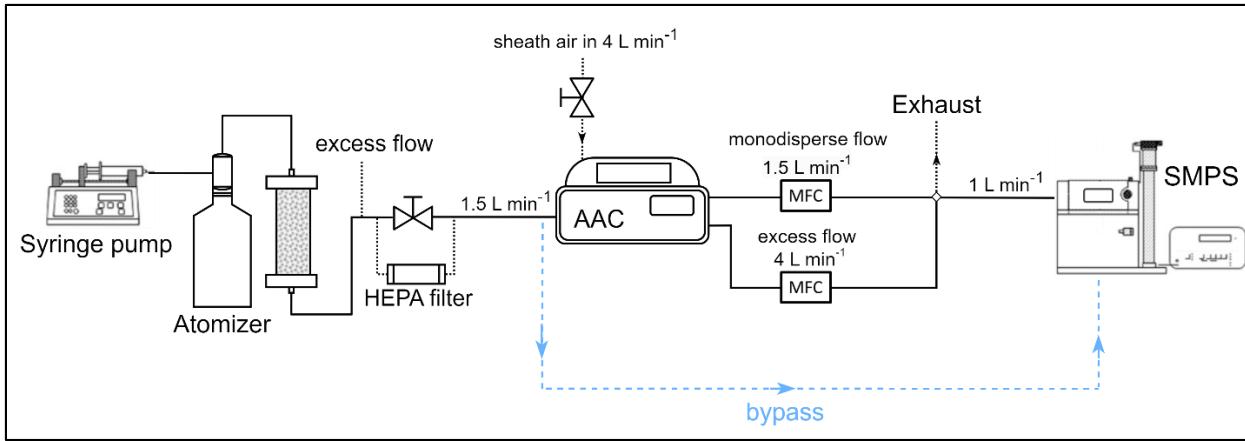
Figure S3. Experimental set-up to assess the losses through the MFCs using ammonium sulfate containing particles 5 g L^{-1}.
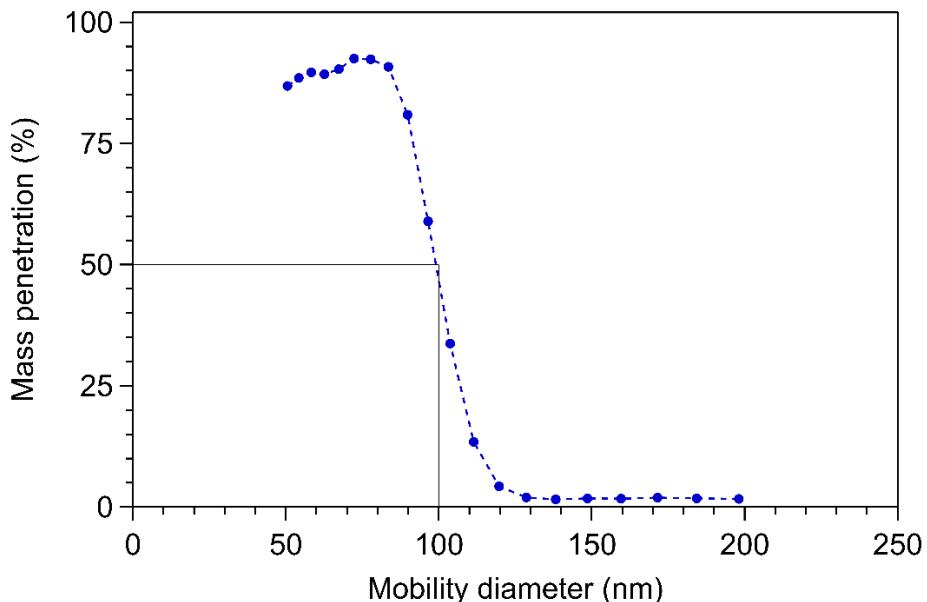
Figure S4. Mass penetration percentage of $PM_{0.1}$ measured by the SMPS for the experimental set-up of Figure S3. The dashed line represents the best-fitting curve. The black lines show that the cut diameter (d_{50}), where there is 50% mass penetration, is at 100 nm.
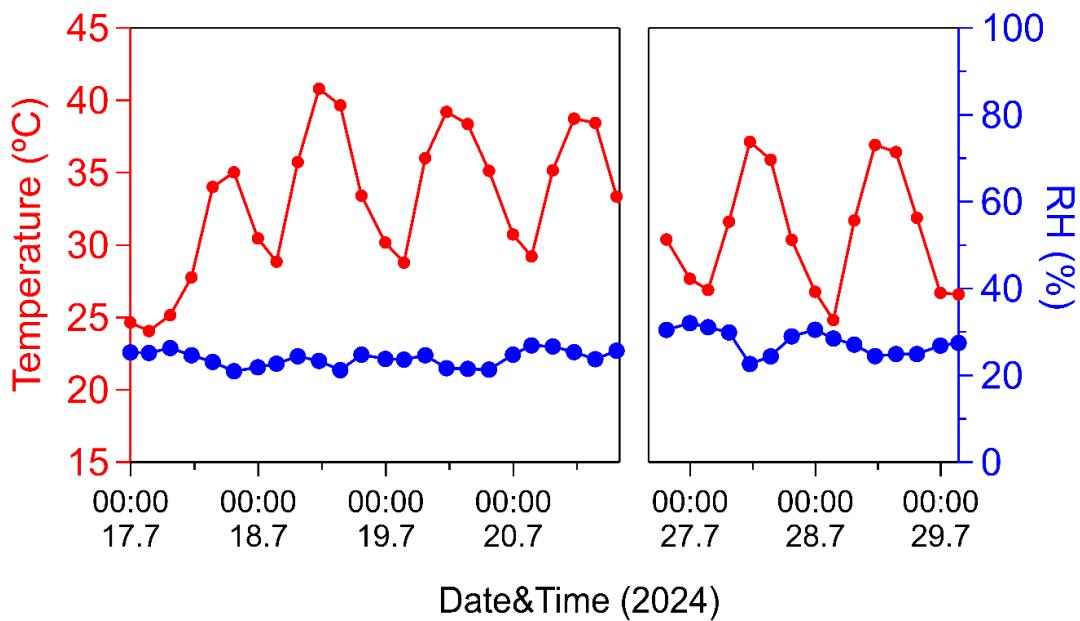
21

22   **Figure S5.** Timeseries of ambient temperature (red, left axis) and relative humidity (RH; blue,
23   right axis) as measured by the Xact625i meteorological sensors.

24

25

26

27

28
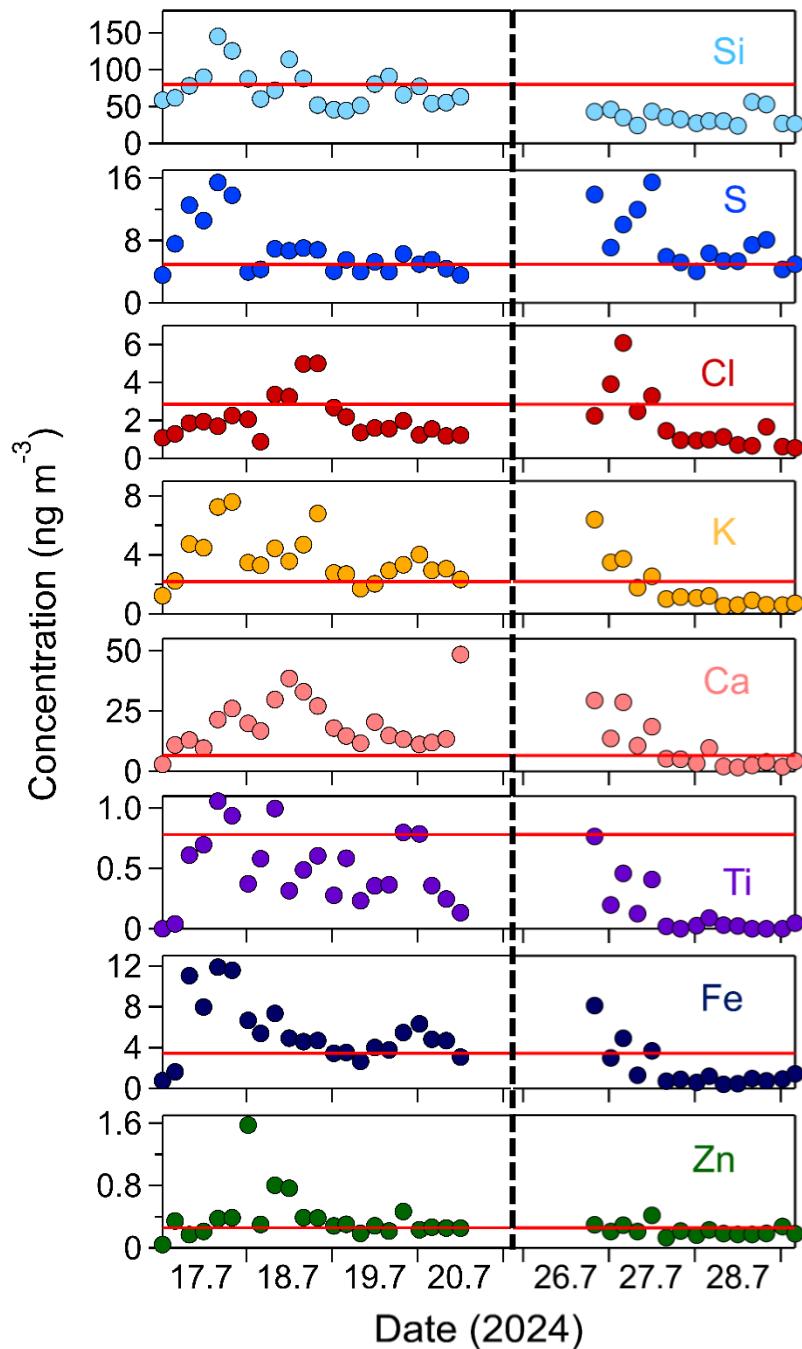
Figure S6. Time series of the uncorrected measurements for the elements detected by the Xact625i, in Patras, Greece, from 17 to 29 July 2024. Each point represents a 4-hour sample. The red lines represent the limit of detection of each element for 90% confidence level calculated by Eq. (2), and the vertical dashed line indicates the time gap between the measurements.
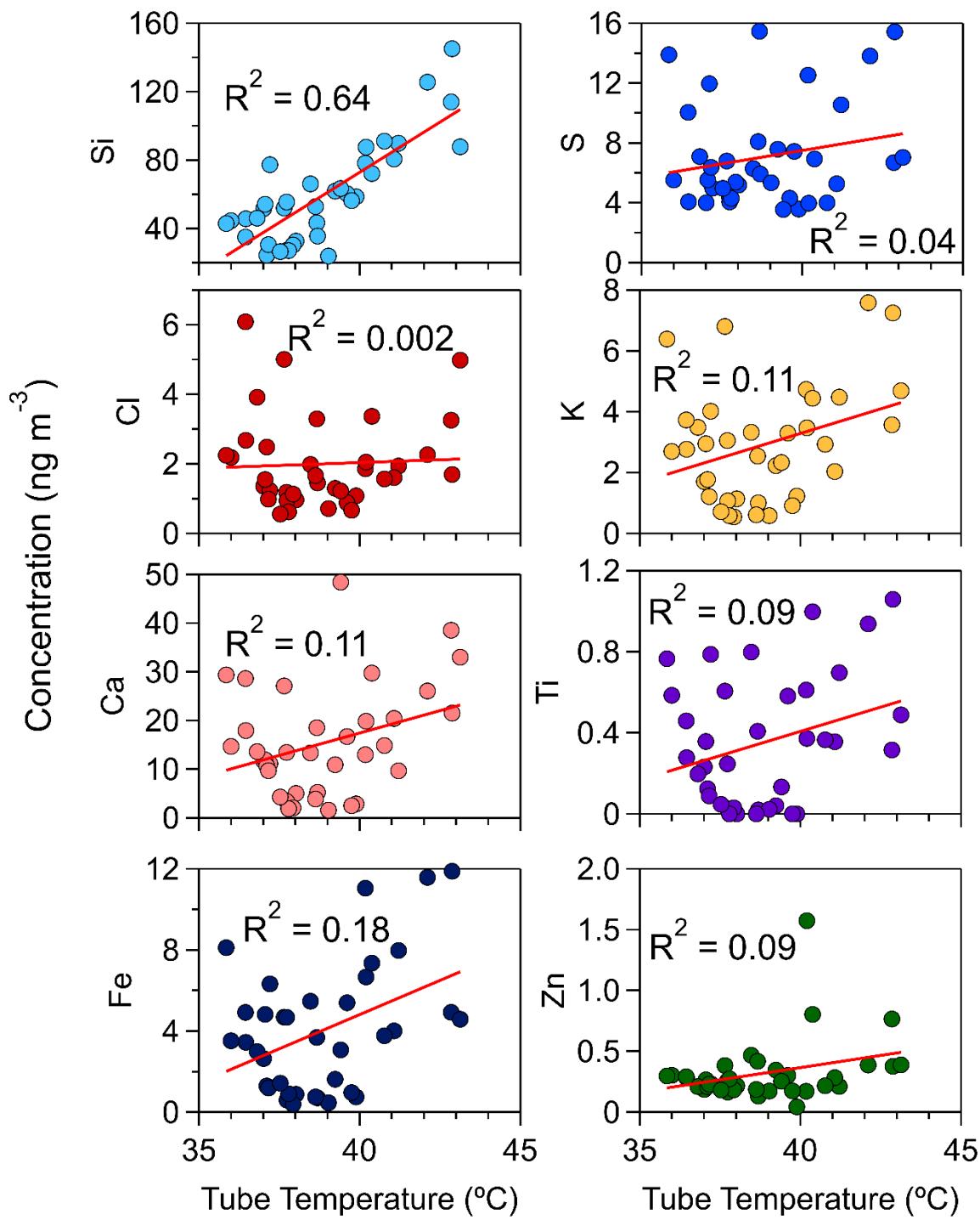
34 **Figure S7.** Uncorrected concentrations of the elements detected by the Xact625i versus the tube
35 temperature of the Xact625i for the measurements in Patras, Greece, from 17 to 29 July 2024.
36 Each point represents a 4-hour sample. The R^2 is also shown.

38
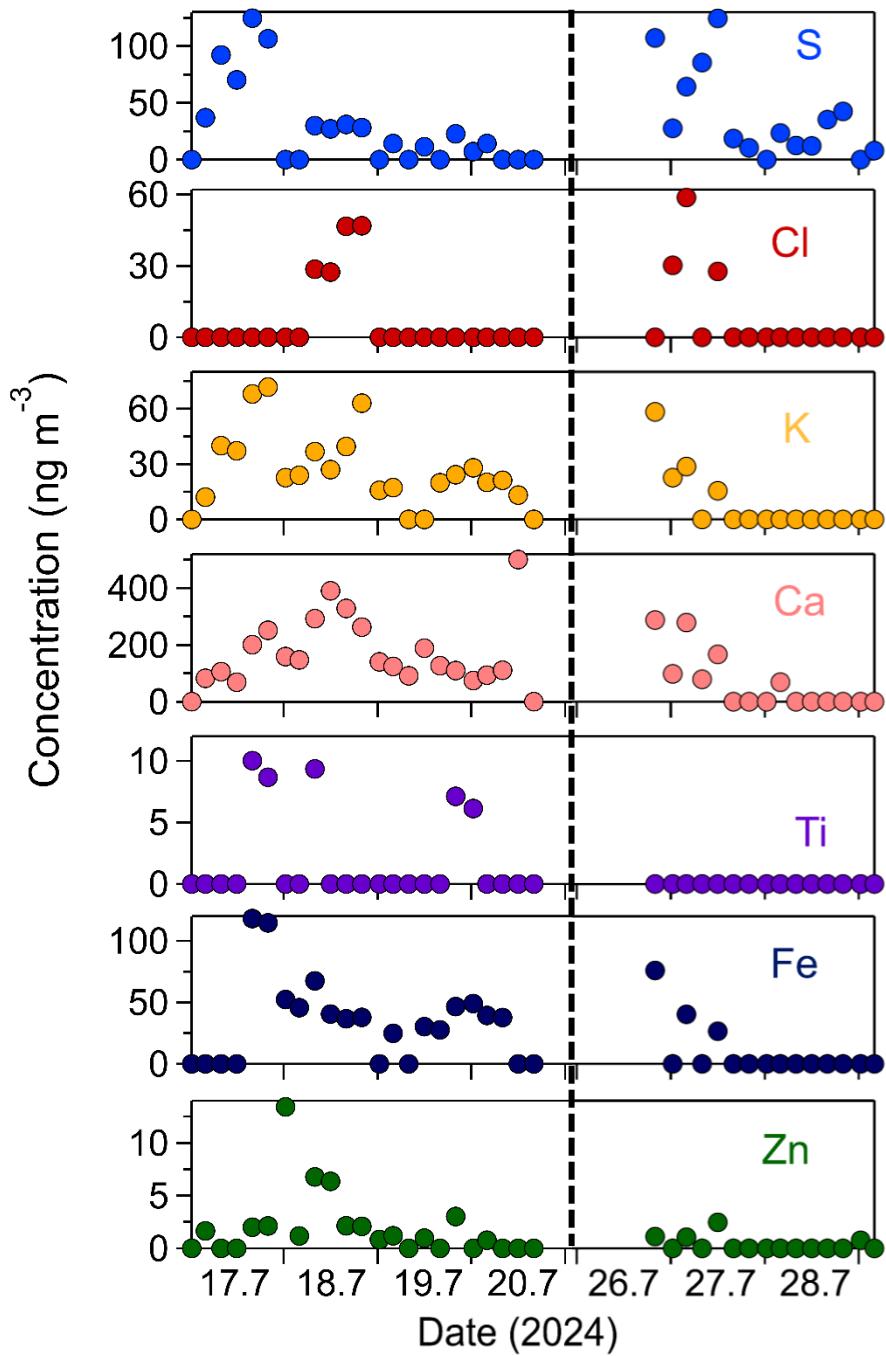
Figure S8. Time series of the corrected measurements for the elements detected by the Xact625i, in Patras, Greece, from 17 to 29 July 2024. Each point represents a 4-hour sample. The vertical dashed line indicates the time gap between the measurements.

42

43

44
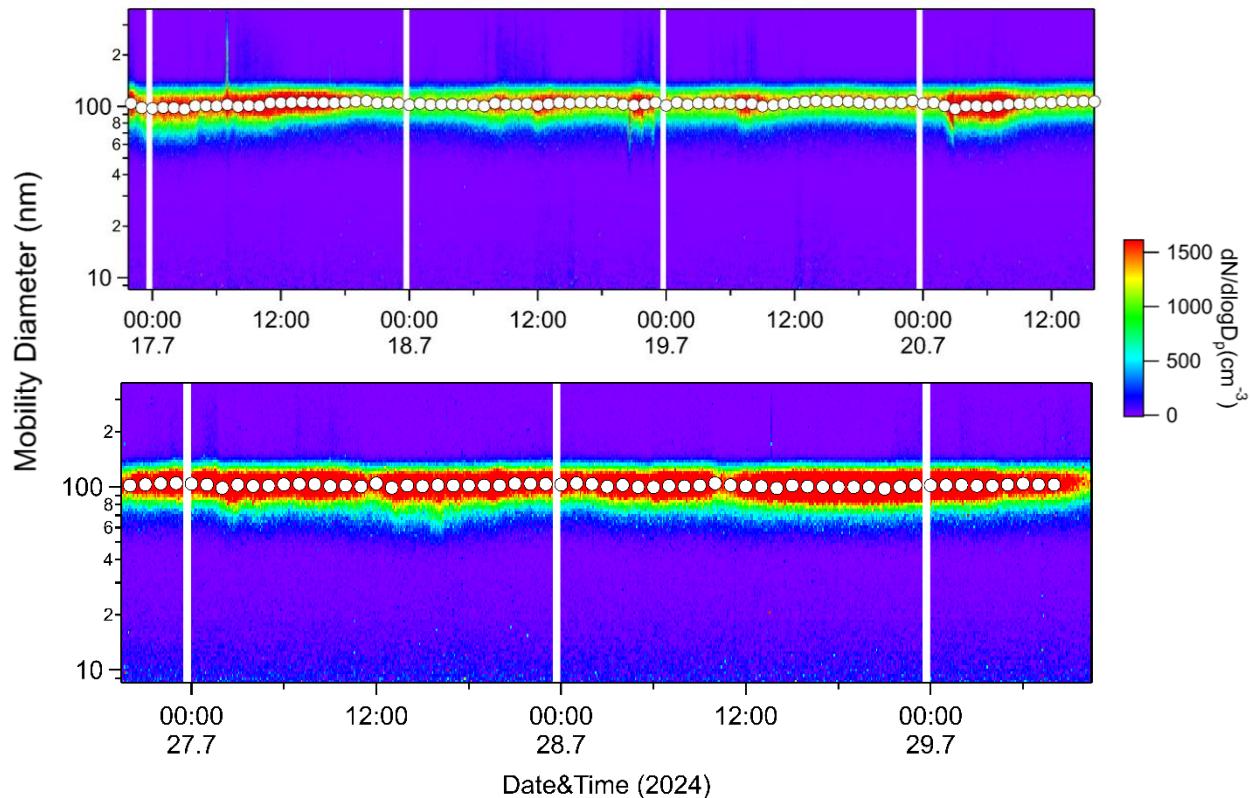
Figure S9. The monodisperse particle number size distributions measured by the SMPS-2 through
time for the ambient measurements in Patras, Greece, from 17 to 29 July 2024. The white round
points indicate the hourly mean diameter (d_{mo}) of the peaks of the monodisperse distributions.

48

49
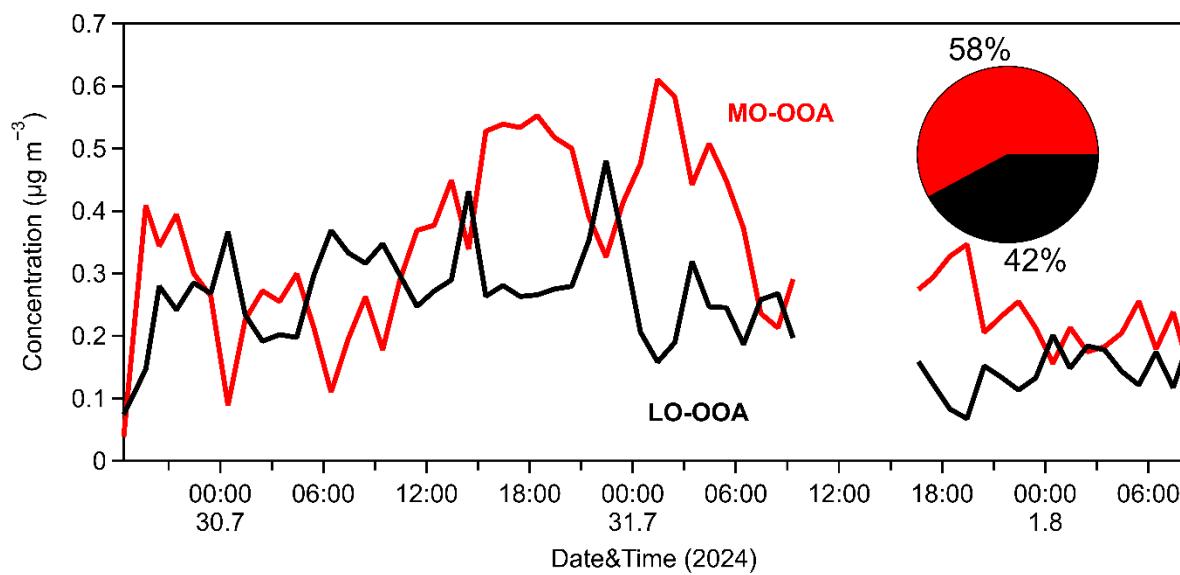
Figure S10. Hourly time-series of the PMF 2 factor solution for $PM_{0.1}$ OA.
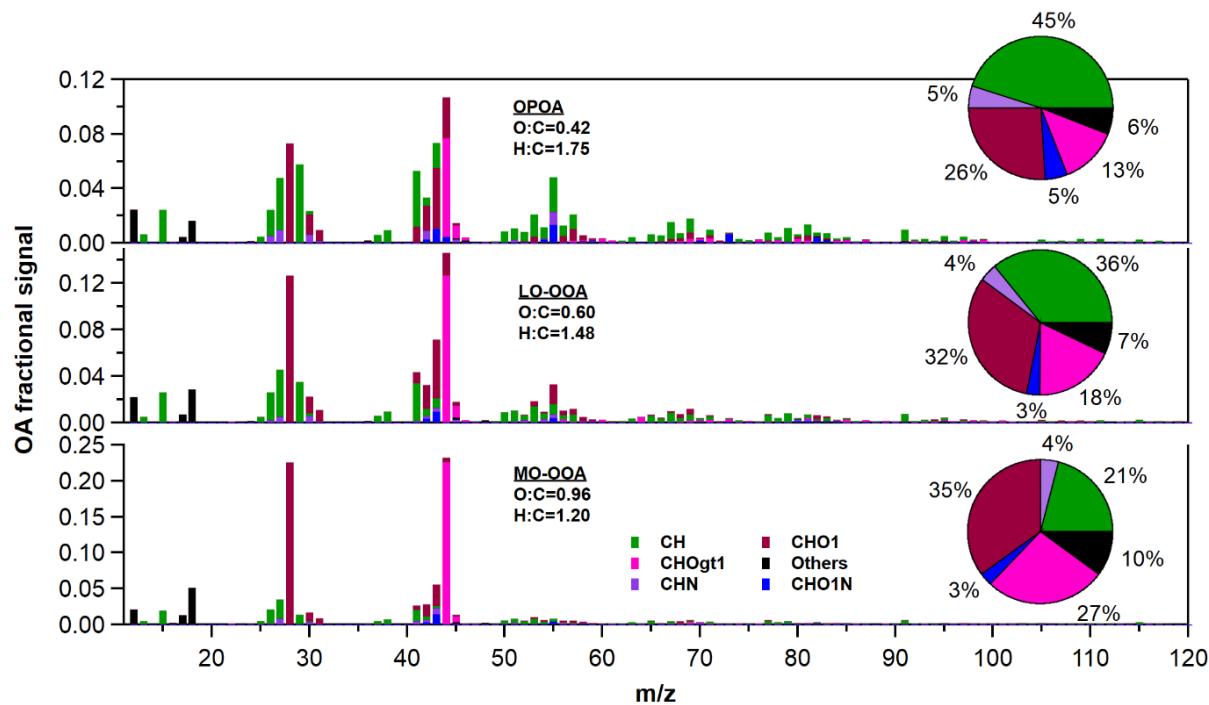
Figure S11. AMS spectra for PM$_{0.1}$ OA PMF factors. Inset pie charts represent the relative contributions of the families, as obtained by analysis of the high-resolution mass spectra.
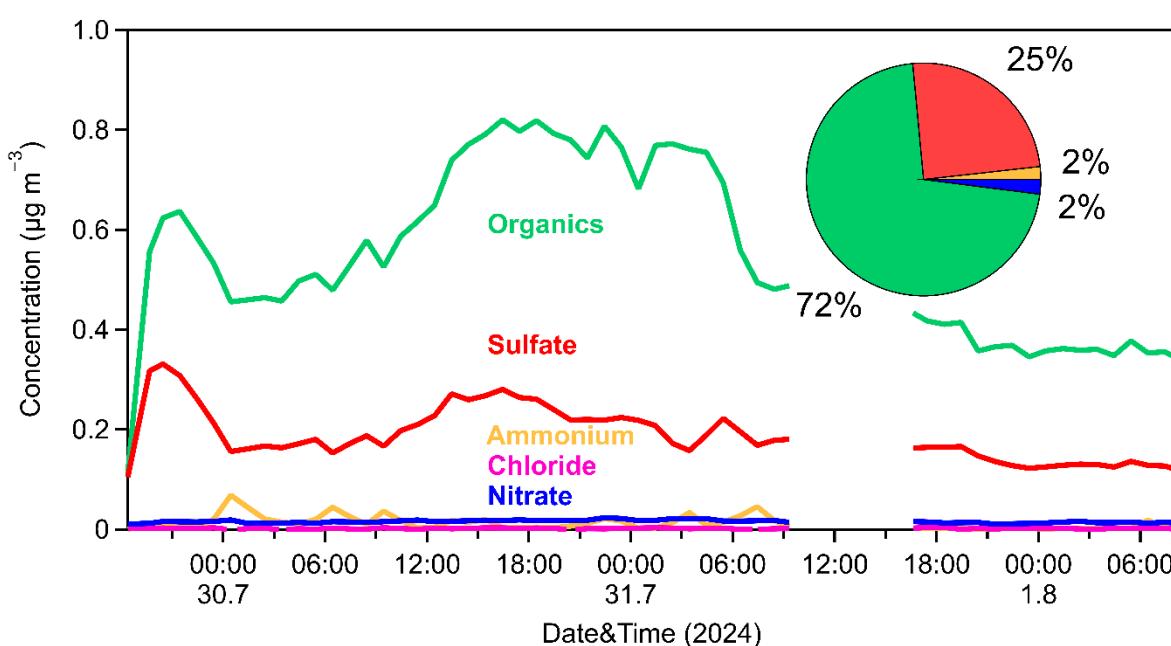
Figure S12. Time series of PM$_{0.1}$ AMS species during the 3-day period.

58

59
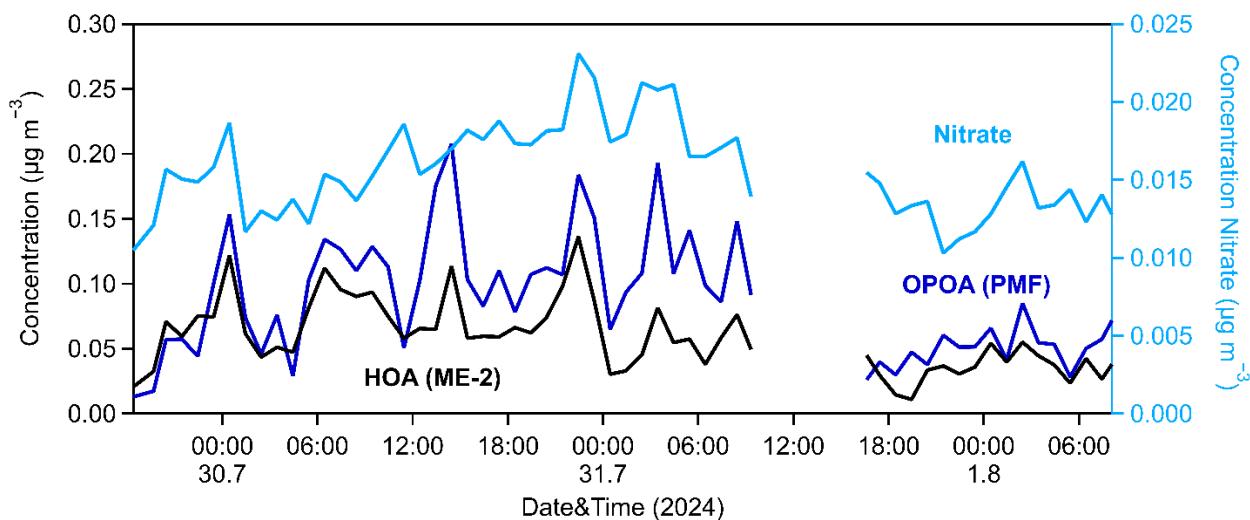
Figure S13. Time-series of nitrate (light blue) (right y-axis) and HOA/OPOA (black/blue) (left y-axis) for the three-day period.

62

63
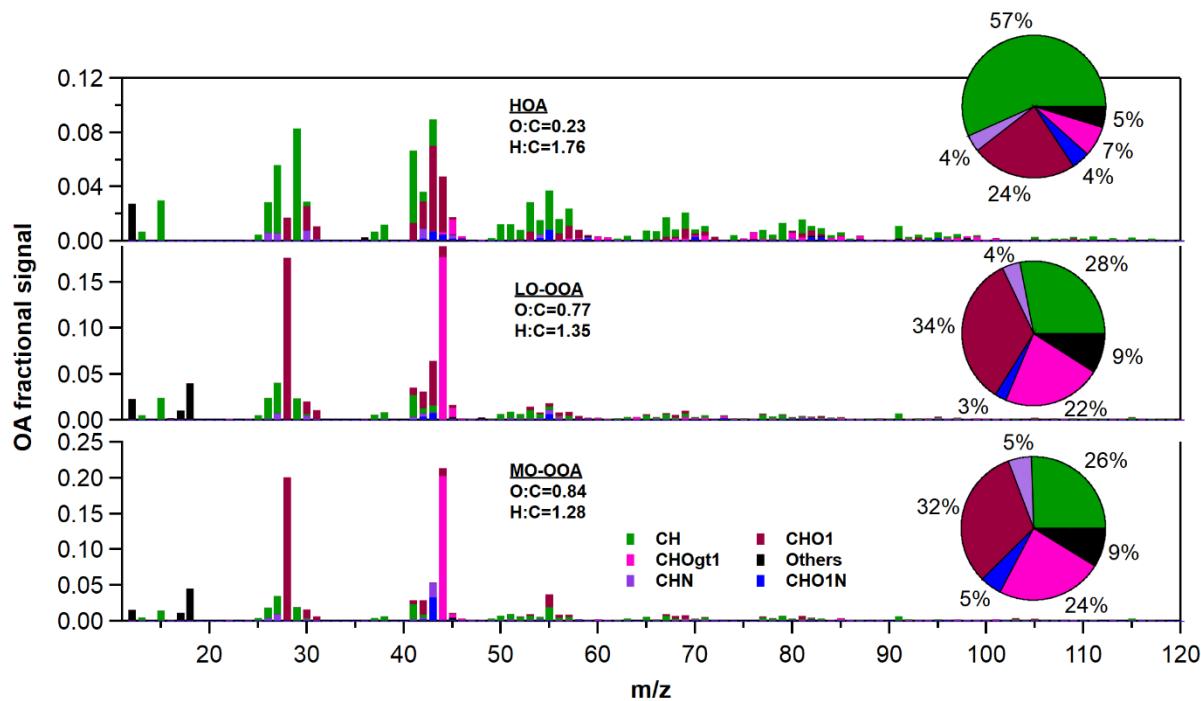
Figure S14. AMS spectra for PM$_{0.1}$ OA ME-2 factors. Inset pie charts represent the relative contributions of the families, as obtained by analysis of the high-resolution mass spectra.

66

Figure S15. Time-series of HOA and OPOA for the three-day period.

67

68

69

70

71

Figure S16. f_{44} vs. f_{43} plot for the PMF factors from this study.

72

73